AD-A113 152 VISIDYNE INC BURLINGTON MA F/G 14/2
PRELIMINARY LABORATORY MEASUREMENTS OF THE BOSS MODULATION TRAN--ETC(U)
JUN 81 T F ZEHNPFENNIG, S A RAPPAPORT F19628-79-C-0005
UNCLASSIFIED VI-604 NL

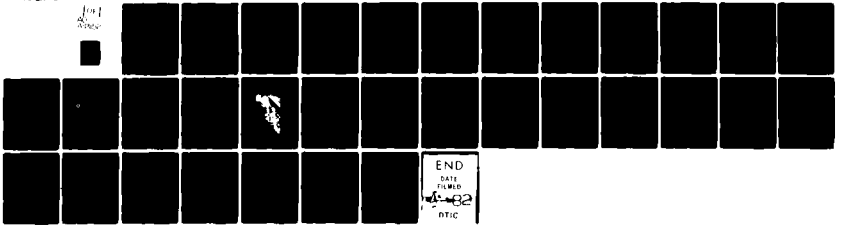

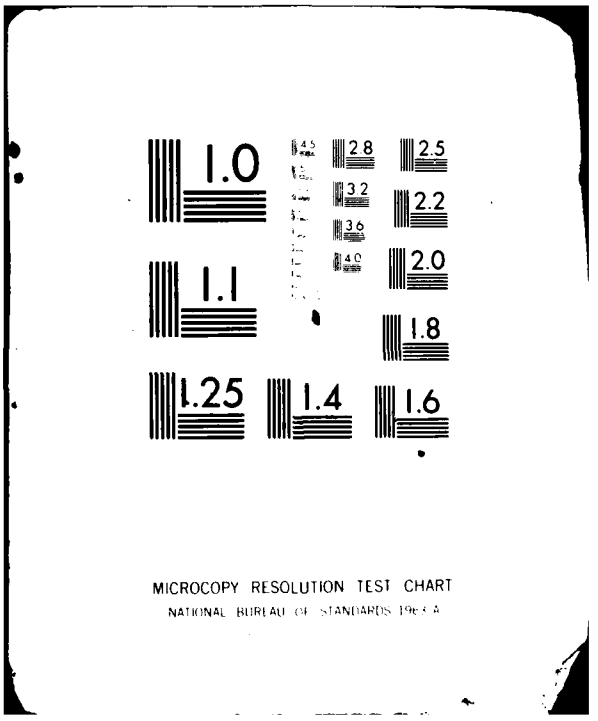
1.0
1.1
1.25
1.4
1.6
1.8
2.0
2.2
2.5
2.8
3.2
3.6
4.0
MICROCOPY RESOLUTION TEST CHART
NATIONAL BUREAU OF STANDARDS 1963-A

(12)

AD A113152

AFGL-TR-81-0156

PRELIMINARY LABORATORY MEASUREMENTS OF THE BOSS MODULATION TRANSFER FUNCTION

T. F. Zehnpfennig
S. A. Rappaport

Visidyne, Inc.
5 Corporate Place
So. Bedford Street
Burlington, Massachusetts 01803

Scientific Report No. 6

5 June 1981

Approved for public release; distribution unlimited

AIR FORCE GEOPHYSICS LABORATORY
AIR FORCE SYSTEMS COMMAND
UNITED STATES AIR FORCE
HANSCOM AFB, MASSACHUSETTS 01731

UNCLASSIFIED

SECURITY CLASSIFICATION OF THIS PAGE (When Data Entered)

REPORT DOCUMENTATION PAGE

READ INSTRUCTIONS BEFORE COMPLETING FORM

1. REPORT NUMBER: AFGL-TR-81-0156	2. GOVT ACCESSION NO.: AD-A113 152
3. RECIPIENT'S CATALOG NUMBER: VI-604	
4. TITLE (and Subtitle): Preliminary Laboratory Measurements of the BOSS Modulation Transfer Function	5. TYPE OF REPORT & PERIOD COVERED: Scientific Report #6
	6. PERFORMING ORG. REPORT NUMBER
7. AUTHOR(s): T.F. Zehnpfennig, S.A. Rappaport	8. CONTRACT OR GRANT NUMBER(s): F19628-79-C-0005
9. PERFORMING ORGANIZATION NAME AND ADDRESS: Visidyne, Inc., 5 Corporate Place, So. Bedford Street, Burlington, MA 01803	10. PROGRAM ELEMENT, PROJECT, TASK AREA & WORK UNIT NUMBERS: 62101F, 767010AD
11. CONTROLLING OFFICE NAME AND ADDRESS: Air Force Geophysics Laboratory, Hanscom AFB, Massachusetts 01731, Contract Monitor: J.A. Sandock/OPR	12. REPORT DATE: June 5, 1981
	13. NUMBER OF PAGES: 33
14. MONITORING AGENCY NAME & ADDRESS (if different from Controlling Office)	15. SECURITY CLASS. (of this report): Unclassified
	15a. DECLASSIFICATION/DOWNGRADING SCHEDULE

16. DISTRIBUTION STATEMENT (of this Report)

Approved for public release; distribution unlimited.

17. DISTRIBUTION STATEMENT (of the abstract entered in Block 20, if different from Report)

18. SUPPLEMENTARY NOTES

This research was partially sponsored by the Air Force Space Division under Line Item 0002 of Contract F19628-79-C-0005.

19. KEY WORDS (Continue on reverse side if necessary and identify by block number)

Background suppression, spatial filter, spatial filtering, background clutter

20. ABSTRACT (Continue on reverse side if necessary and identify by block number)

A dual-input radiometer with matched modulation transfer functions is described. The two MTF's are defined by the form of the two entrance pupils, one of which is annular and the other of which is circular. The radiometer switches alternately between the two pupils by means of a set of polarizing components. By detecting only the resulting fluctuations in the image, the lower sptaial frequencies in the object scene are suppressed. Preliminary measurements of the suppression characteristics as a function

DD FORM 1 JAN 73 1473 EDITION OF 1 NOV 65 IS OBSOLETE

UNCLASSIFIED

SECURITY CLASSIFICATION OF THIS PAGE (When Data Entered)

of spatial frequency are presented.

TABLE OF CONTENTS

LIST OF FIGURES

1.0 INTRODUCTION

The work described in this Technical Report was performed under Contract F19628-79-C-0005. The purpose of this program was to design, fabricate, and test a laboratory breadboard of a dual channel IR radiometer having tailored modulation transfer functions. The MTF's of the two optical channels were to be matched to suppress as completely as possible all spatial frequencies in the object below approximately 25% of the cutoff frequency.

The Background Optical Suppression System (BOSS), which has been described in various forms in References 1 through 6, uses pairs of matched modulation transfer functions to suppress the range of lower spatial frequencies in a structured background, thereby enhancing the detectability of point sources or targets seen against that background. The MTF pairs are tailored to match as closely as possible at low spatial frequencies, but must diverge significantly from each other at higher frequencies. Then, by detecting only fluctuations when the two images corresponding to these two MTF's are alternately projected onto the common detector plane, the MTF's are, in effect, subtracted from one another and the lower spatial frequencies in the object are suppressed.

The program began with an initial definition phase in which various design options were examined:

A. Alternative methods for switching from one optical channel to the other were examined, and the most promising one selected for this application.

B. Suppression characteristics of various tailored MFT systems (particularly, matched pairs of circular and annular apertures) were examined and the most promising pair for this application chosen.

C. Geometry trade-offs (aperture diameter vs focal length vs detector size) were evaluated in order to optimize the dimensions of the laboratory model.

D. Evaluation and specification of detector and electronics for laboratory model were performed.

E. Methods for fine-tuning the optical system to achieve final matching of the MTF's and effective collecting areas were examined.

Following the initial definition phase, detailed design and fabrication of the radiometer was performed.

The final phase consisted of a program of laboratory measurments to determine the maximum suppression ratio (as a function of spatial frequency) which can be achieved with this instrument. At this time, only preliminary measurements of the optical system response at three spatial frequencies are available. These measurements show that the instrument behaves qualitatively as expected. At a spatial frequency of zero, a suppression ratio in excess of 100 was achieved. At a relatively high spatial frequency (59% of the way to cutoff), no suppression was observed, as expected. At a spatial frequency 11.8% of the way to cutoff, in the region where effective suppression was expected, a suppression ratio of about 7 was observed. The suppression ratio here was probably limited by certain shortcomings of the present apparatus, which are discussed in Section 4. Suppression ratios at lower spatial frequencies which are at least an order of magnitude higher than this should be achievable with additional work.

A condensed version of this report was presented at the 1981 Los Angeles Technical Symposium, sponsored by the Society of Photo-Optical Instrumentation Engineers (SPIE), and will be published in SPIE Proceedings Number 268.

In the course of this work, a novel technique for achieving a matched set of MTF's in optical systems with a single entrance pupil was conceived and investigated in a preliminary manner. The matched MTF's are produced by causing the image to undergo a programmed sequence of high-frequency, small amplitude gyrations on the detector face. This technique was described in a paper presented at the SPIE'S 24th Annual Technical Symposium and was published in SPIE Proceedings Number 253. This paper is reproduced in the Appendix.

Section 2.0 describes the initial definition phase of this program, in which the various design options were examined.

Section 3.0 describes the laboratory apparatus which was constructed.

Section 4.0 describes the preliminary measurements which have been made using this apparatus.

2.0 DEFINITION PHASE

During the Definition Phase, the various design options listed in Section 1.0 were evaluated, and the alternatives most appropriate for this program were selected. The following paragraphs describe that selection process.

The method chosen for switching from one entrance pupil to the other used an arrangement of rotating and stationary polarizing components shown in Figure 1. First, the radiation from the source entering the entrance pupils was linearly polarized. A quartz half-wave plate over one of the two pupils then rotated the plane of polarization for this pupil by 90°. Then, a rotating analyzer prism in front of the detector alternately passed the polarized radiation from one pupil and then the other, with smooth transitions in between. This part of the apparatus is more completely described in Section 3. Other switching techniques involving rotating apertures, solenoid operated shutters, and tilting mirrors were considered. The advantage of the polarization technique over the others is that the transitions are performed smoothly, without disturbing transient effects or momentary changes in the shapes and/or sizes of the pupils during the switching phase. The polarization method is, of course, wasteful in its use of the incident radiation. However, the main objective here was to accurately watch the MTF's at low spatial frequencies, and efficient use of the incident radiation was considered to be less important in this phase.

The wavelength of the center of the radiometer spectral passband was chosen to be 2.0 μm because this was the longest wavelength for which the fabricator of the half-wave plate had reliable data on the retardation value of crystalline quartz. Also, 2.0 μm is a convenient wavelength at which to work because satisfactory optical materials and suitable detectors are readily available, and absorption by atmospheric gases is not a problem.

From among the various possible pairs of matched MTF's described in the references, the pair consisting of a diffraction-limited annulus and a smaller diffraction-limited circular pupil was chosen, as shown in Figures 2 and 3. This was considered to be the simplest and most easily implemented arrangement which could provide

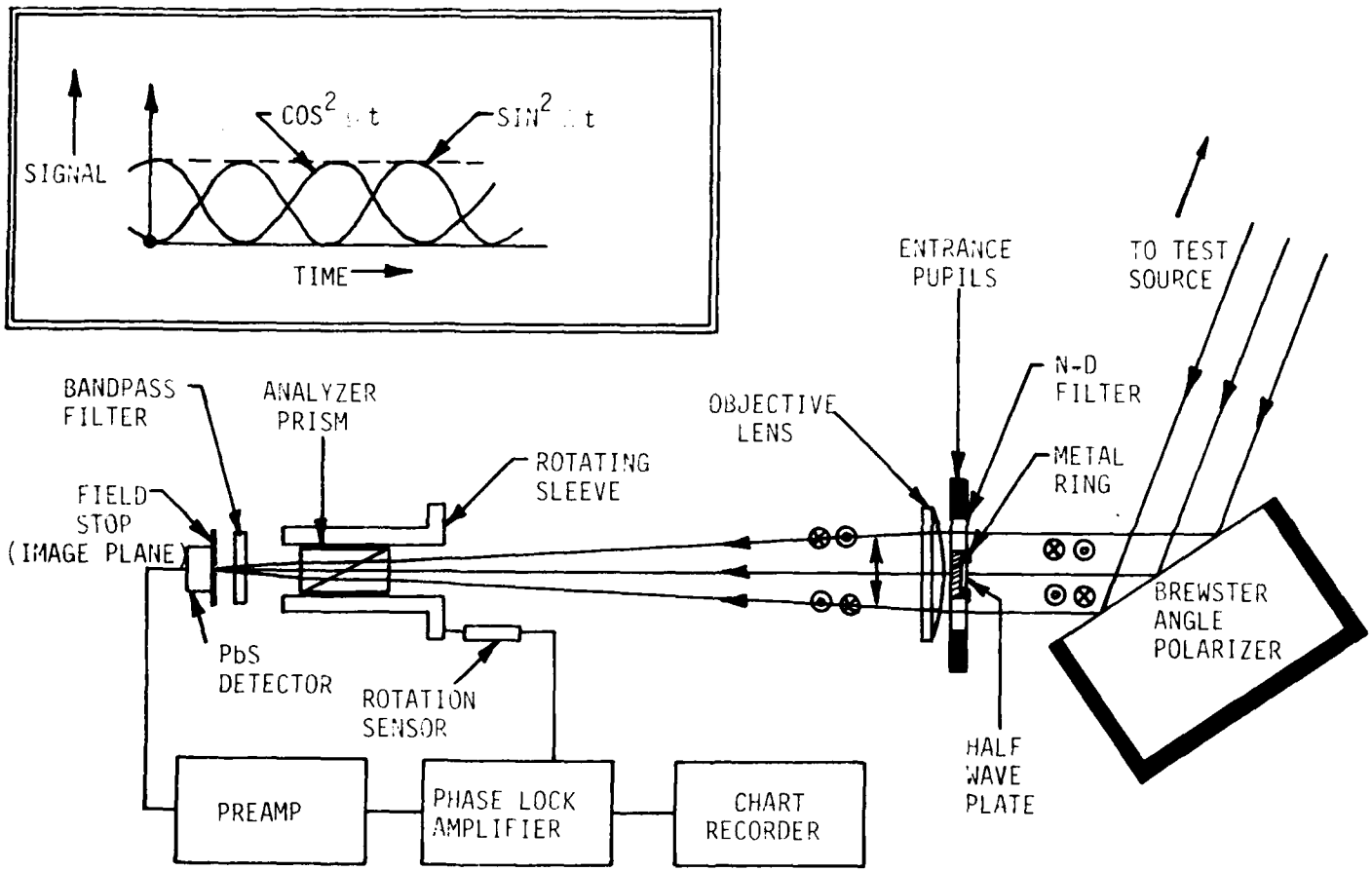

Figure 1. Schematic diagram of the radiometer and Brewster angle polarizer.

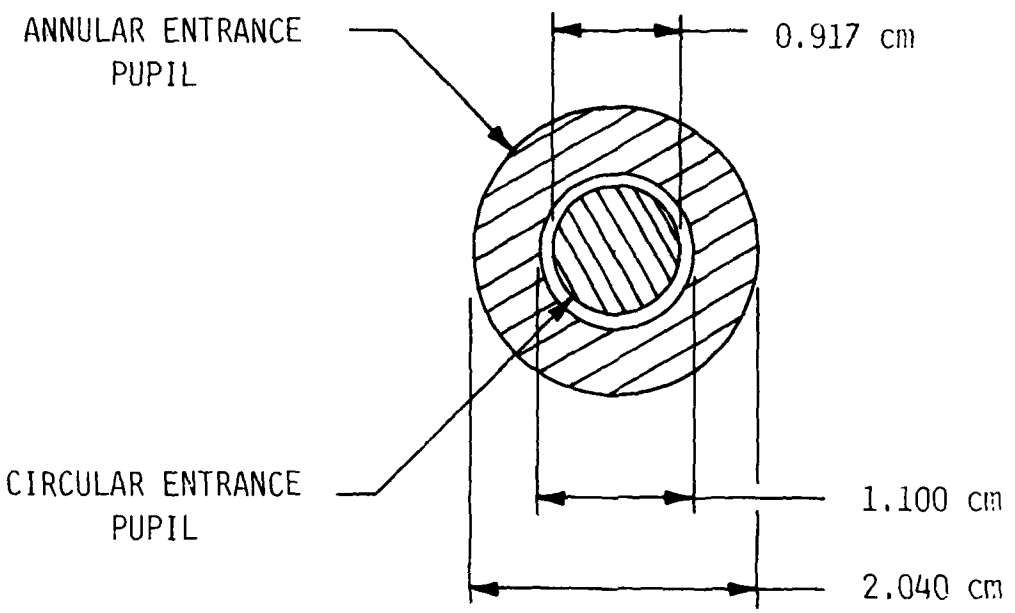

Figure 2. Dimensions of the two entrance pupils.

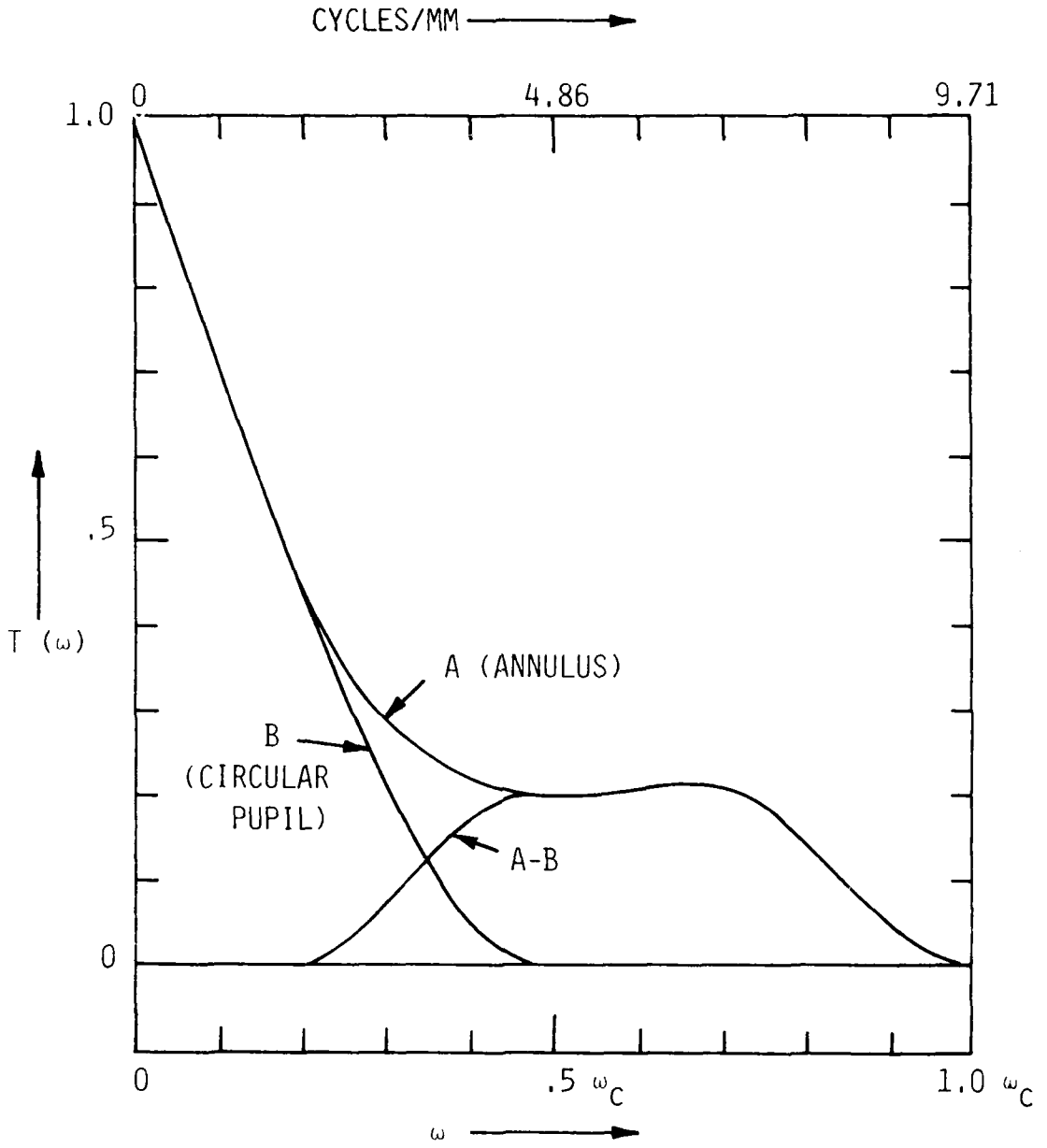

Figure 3. Matched set of modulation transfer functions corresponding to the entrance pupils shown in Figure 2.

good suppression over a reasonable range of lower spatial frequencies. The area of the annular pupil is several times that of the circular pupil, thus requiring that a neutral density filter be placed over the annulus to equalize the effective collecting areas. Once again, efficient use of the incident illumination was not considered important in this laboratory program.

With regard to the geometry trade-offs (aperture diameters vs focal length vs detector size), the approximate aperture of the circular pupil was constrained by the 10 mm diameter of readily available half-wave plates. Then, the requirement that the MTF's match accurately out to about 25% of the cutoff frequency determined the approximate dimensions of the annulus. The outside diameter of the annulus used here was 2.040 cm. For a number of reasons, a relatively long focal length for the objective lens is desirable. With a long focal length, the effects of geometric aberrations of the lens, such as spherical aberration, are decreased. Also, the size of the diffraction-limited point spread function increases with the focal length, allowing a larger field stop diameter and relaxing the mechanical precision required from the spatial scan mechanism. Also, the depth of focus increases with the focal length. For these reasons, a focal length between 100 and 200 cm seemed appropriate. A single element, plano-convex lens with a focal length of 105 cm was finally selected. In order to define shape and size of the field of view, a circular field stop aperture was placed in the image plane, just in front of the detector. The diameter of the field stop opening involved a tradeoff between signal level, which increases with the diameter, and contrast in the spatial scans of the higher frequency test targets, which decreases with field stop diameter. It seemed reasonable to choose a field stop diameter such that the first zero in the detector transfer function would approximately coincide with the cutoff frequency in the MTF of the diffraction-limited annulus. The resulting field stop diameter was 100 microns. This size proved to be small enough to give reasonable contrast in scans of the higher frequency test targets (such as the target with a spatial frequency 59% of cutoff), while at the same time yielding adequate signal

levels. The field stop consisted of a thin disk of nickel foil containing the 100 micron opening. The disk was centered on the detector and then tacked in place around the edges with an adhesive.

The detector chosen for these measurements was a Quantum-Detector Technology, Inc., 100 x 100 micron PbS detector. This choice was made because this detector is readily available, its characteristics are familiar to Visidyne personnel, and it works well at 2 microns. Because the objectives of this program involved the optical properties of the instrument, no attempt was made to choose "realistic" detector electronics as would be used in an actual flight system containing a detector array with a large number of elements. Instead, near-ideal electronics were used, in the form of a Princeton Applied Research Phase Lock Amplifier, Model 126. The polarity of this amplifier was switched synchronously with the rotation of the analyzer prism. In this way, the output of this amplifier was made proportional to the cross-correlation of the actual detector signal with a square wave having the same frequency and phase as the expected detector signal. This is probably the optimum method for extracting a periodic signal from a noisy background.

The methods for fine-tuning the optical system to achieve close matching of the MTF's at lower spatial frequencies involved varying the outside diameter of the annulus and also adjusting the effective collecting area of the annulus by adjusting the tilt angle of a thin metal vane. As stated previously, the effective collecting areas of the two pupils were roughly matched by placing an N-D 0.50 filter over the annulus. Nominally, this left the effective collecting area of the annulus about 9% greater than that of the circular pupil. Final matching was performed by obscuring a portion of the area of the annulus with the thin metal vane, as shown in Figure 4. The amount of obscuration could be controlled precisely by tilting the vane. (The long dimension of this vane was oriented perpendicular to the direction of the lines in the test targets, so that its effect on the shape of the observed MTF of the annulus would be minimized.) This matching was performed with the uniform test target (zero spatial frequency) in place. It was then planned to observe the amount of suppression at some higher spatial frequency within the region of

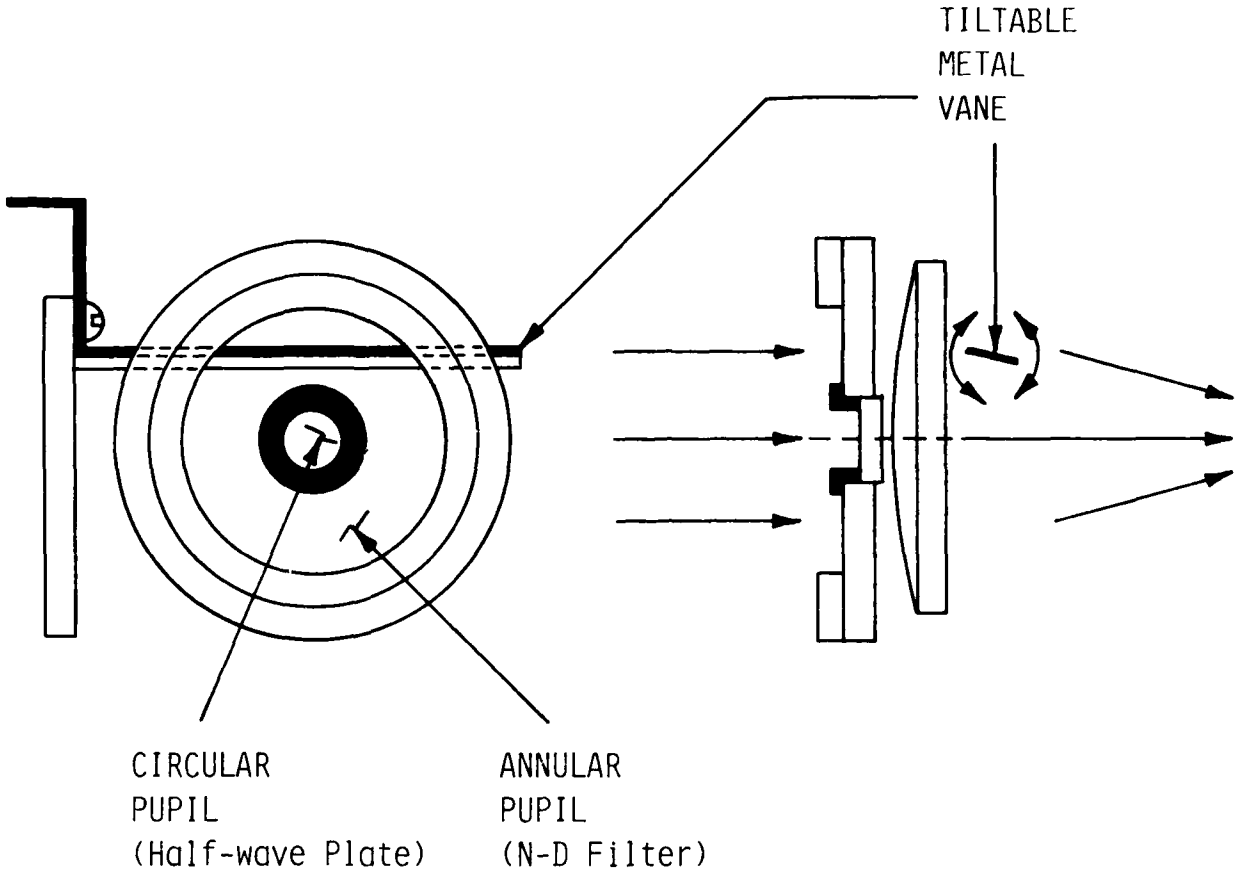

Figure 4. Entrance Pupil Assembly, with metal vane for fine adjustment of the effective collecting area of the annulus.

suppression, such as at 20% of cutoff. From the amplitude and phase of the residual (unsuppressed) fundemental spatial frequency, a corrected value for the outside diameter of the annulus could be computed. The O.D. would then be so modified. (The stop which determined the O.D. of the annulus was fabricated in several slightly different sizes.) Then, the matching at zero spatial frequency would be repeated, the suppression at 20% of cutoff would be measured again, and the process repeated until suitable low-frequency matching of the MTF's was observed. Due to problems discussed in Section 4, this process has not yet been carried out in its entirety.

3.0 THE APPARATUS

The tailored modulation transfer functions were produced by matching a diffraction-limited circular entrance pupil to a larger diffraction-limited annular pupil. Given an annulus with an outside diameter of unity, it was found that a suitably matched pair of MTF's will result if the outside diameter of the circular pupil is set equal to 0.450 and the inside diameter of the annulus is set equal to 0.540. The calculated MTF's for this combination are shown in Figure 3. The matching is very good out to 20% of the cutoff frequency, ω_c, of the annulus, with the largest calculated mismatch in this range being 0.005 at 10% of ω_c. Beyond 0.45 ω_c, the MTF of the circular pupil (Curve B) drops to zero, and the combined MTF (Curve A minus Curve B) is that of the annulus alone.

The actual dimensions of the entrance pupils used in this radiometer are shown in Figure 2. The two pupils were concentric, as shown, and shared the same objective lens. The nominal value of ω_c referenced to the image-plane of the radiometer is 9.71 cycles/mm, as calculated from the 2.040 cm outside diameter of the annulus, the 105 cm focal length of the objective lens, and the nominal 2.0 micron wavelength of the radiation. The geometric collecting areas of the two pupils were substantially mismatched, with the area of the annulus being 3.50 times that of the circular pupil. This mismatch was corrected in part by placing a metallic neutral density filter with a nominal transmittance of 0.316 (neutral density 0.50) over the annulus.

The major components of the apparatus are shown in Figures 1 and 5. As stated previously, the method chosen for switching alternately between one entrance pupil and the other without producing disturbing transient effects utilized a set of polarizing components. First, incident radiation from the test source was linearly polarized by reflection from an uncoated optical flat set at Brewster's angle, and it then passed through the entrance pupils and the common objective lens. The portion of the radiation passing through the annular pupil was attenuated by the N-D filter, but its state of polarization was not changed. Radiation passing through the circular pupil, however, encountered the half wave plate, which was oriented so

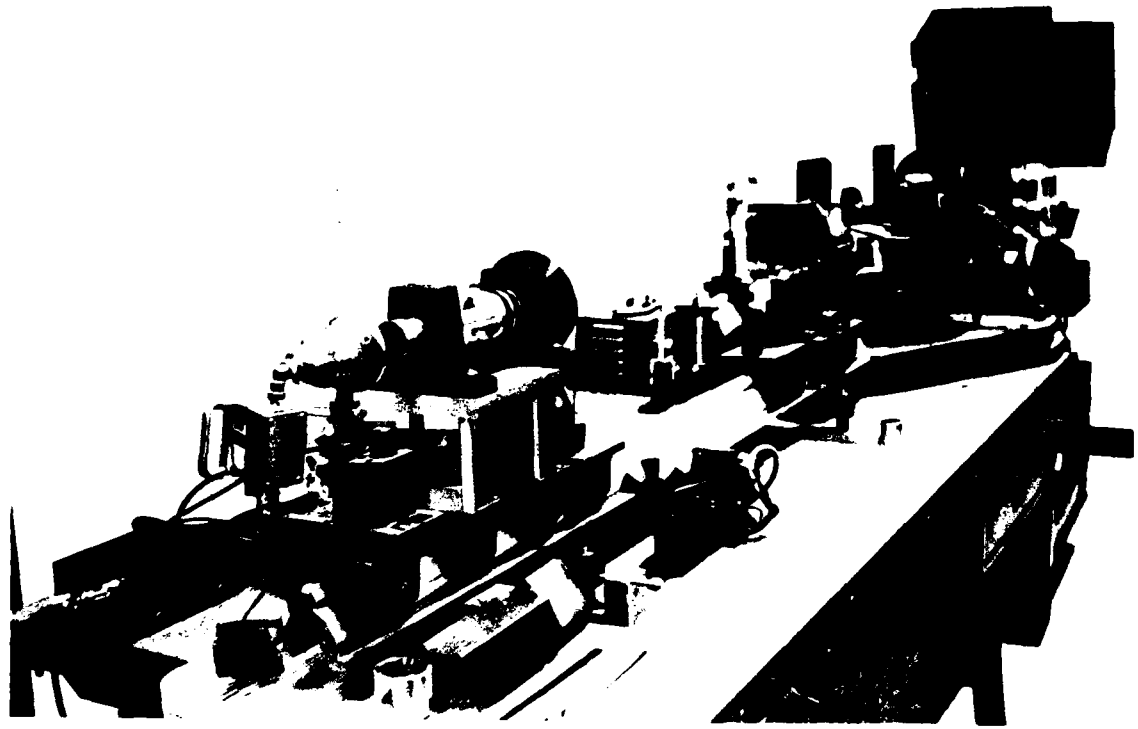

Figure 5. Photograph of the apparatus.

as to rotate the plane of polarization by 90°. (The region between the inside diameter of the annulus and the outside diameter of the circular pupil was blocked by a thin metal ring, as shown). A Glan-Thompson analyzer prism mounted in a rotating sleeve assembly was located just ahead of the image plane. This sleeve, which was driven continuously at 4.67 revolutions/sec by a synchronous motor, rotated about an axis coincident with the optical axis of the radiometer. In this way, the image observed in the plane of the field stop consisted, alternately, of radiation passing through one entrance pupil and then the other pupil, with smooth transitions in between. For instance, if the intensity of the images formed by the two pupils over the field stop opening were identical, the signal corresponding to one entrance pupil would vary as $\sin^2\Omega t$, and of the other as $\cos^2\Omega t$, as shown in the insert in Figure 1. Thus the total signal from the detector would be constant with time, and the output of the phase lock amplifier would be zero. If, on the other hand, the intensities of the images were different, the output of the phase lock amplifier would be proportional to that difference. Switching of the phase lock amplifier was synchronized to the rotation of the analyzer prism with a fiber optic rotation sensor viewing a sector pattern located on the face of the rotating sleeve. The polarity of the amplifier was reversed for each 90° rotation of the prism.

The bandpass filter was an interference filter with bandwidth of 0.04 microns centered on 2.0 microns. It was necessary to restrict the spectral bandpass because the half wave plate produces the required $\lambda/2$ retardation only over a limited spectral range.

The optical path length through the N-D filter (annulus) was longer than the path length through the central pupil (half wave plate) by approximately three times the coherence length of the radiation, as determined by the bandwidth of the interference filter. Thus, the images from the two entrance pupils were combined incoherently in the detector plane, as desired.

The test source, seen in the background of Figure 5, consisted of a set of backlighted Ronchi rulings located in the focal plane of a paraboloidal collimating mirror. Backlighting was provided by a tungsten-halogen lamp used with a condenser system. The Ronchi rulings

were mounted on a motor-driven translation stage, allowing spatial scans of the rulings to be made with time. The spatial frequencies of the rulings, referenced to the image plane of the radiometer, ranged from 1.15 cycles/mm up to 7.66 cycles/mm. An unruled region in the test target plane provided a uniform field with a spatial frequency approaching zero.

A possible future improvement to the apparatus would be to provide a test source having sinusoidal test targets instead of the square-wave (Ronchi) targets used here. The degree of suppression of the fundamental spatial frequency can be determined in a spatial scan of a square-wave target despite the presence of the higher spatial frequency components in that square-wave. However, when the objective is to demonstrate large suppression ratios, it is more convincing if those higher spatial frequencies are entirely absent from the target. Hence, sine wave targets would be desirable.

4.0 PRELIMINARY RESULTS

Initial alignment of the various optical components in the radiometer and test source was performed using a He-Ne laser. The radiometer was then focused by measuring the contrast in the image of one of the higher spatial frequency Ronchi rulings for several image plane positions. The detector assembly was then locked in the plane having the highest contrast. Next, with the analyzer prism turning, the orientation of the half wave plate was adjusted so as to rotate the plane of polarization of the radiation passing through the central pupil by 90°. This was done by blocking off the central pupil and then maximizing the reading of the phase lock amplifier on the signal due to the annulus by varying the phase adjustment on the amplifier. Next, the annulus was blocked, the central pupil was opened, and the phase adjustment of the amplifier was incremented exactly 90°. Then, the half wave plate was rotated to maximize this second reading and locked in place. Finally, with the spatially uniform test target in place, the effective collecting areas of the two pupils were adjusted to give optimum suppression (zero signal) at ω=0. This was done by shadowing a portion of the area of the annulus with a thin metal vane, as previously described.

Figure 6 shows a spatial scan of the uniform region of the test target. The observed signal from the phase lock amplifier is 0.0 $\pm$ 0.03 volts, compared to a signal level of +4.0 volts when the central pupil was blocked and the test target was viewed through the annulus alone. Thus, a suppression ratio in excess of 100 was achieved at ω=0.

Figure 7 shows spatial scans of the 1.15 cycle/mm target with both pupils open (lower curve) and with the annulus alone (upper curve). The fundamental frequency of this test target is 0.118 ω_c, and thus is within the expected region of effective suppression, as seen in Figure 1. The scans do demonstrate substantial suppression, by about a factor of 7. However, suppression ratios at least an order of magnitude higher than this should be achievable. The suppression ratio observed here is probably limited by certain shortcomings in the present apparatus, which are briefly described below.

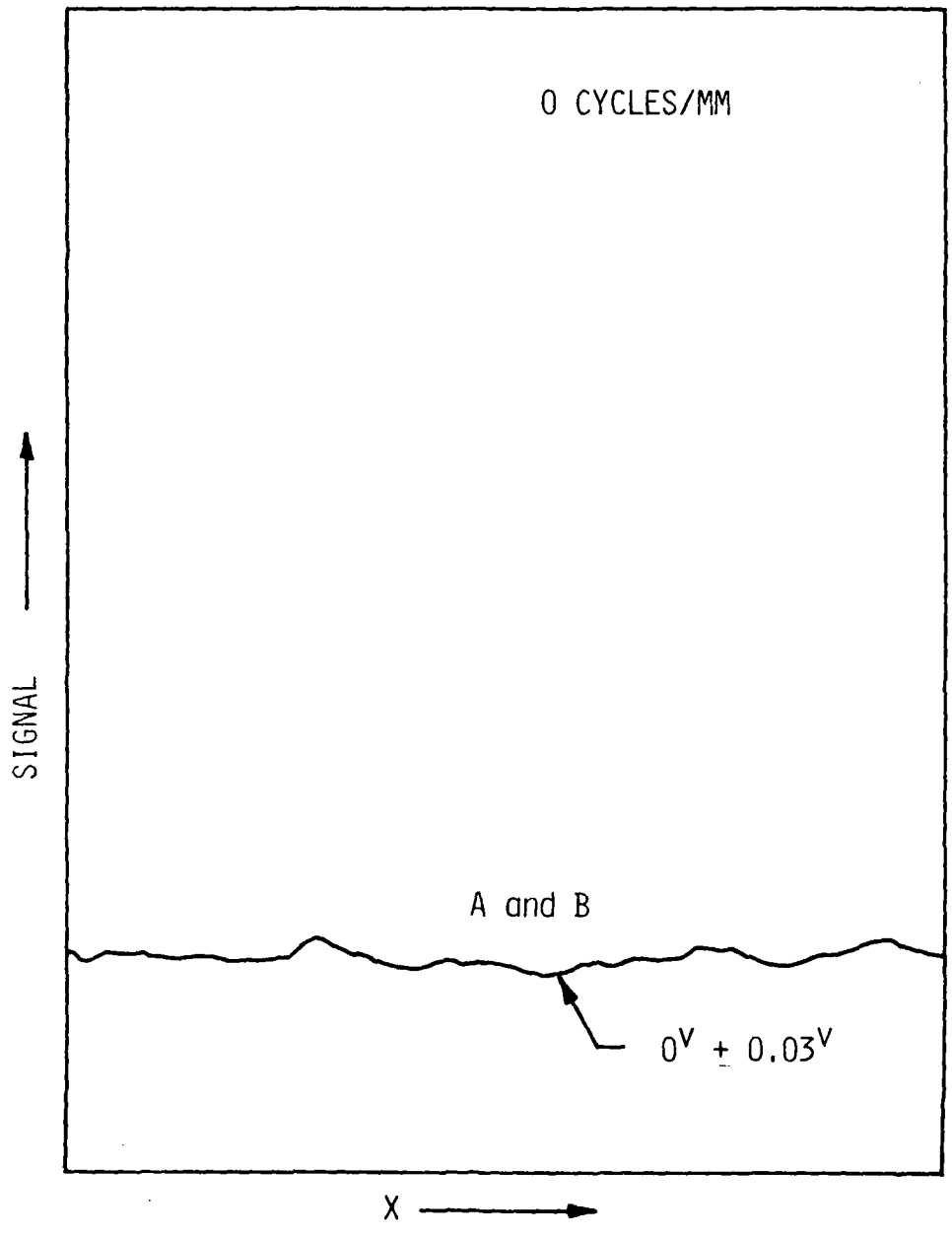

Figure 6. Spatial scan at $\omega = 0$.

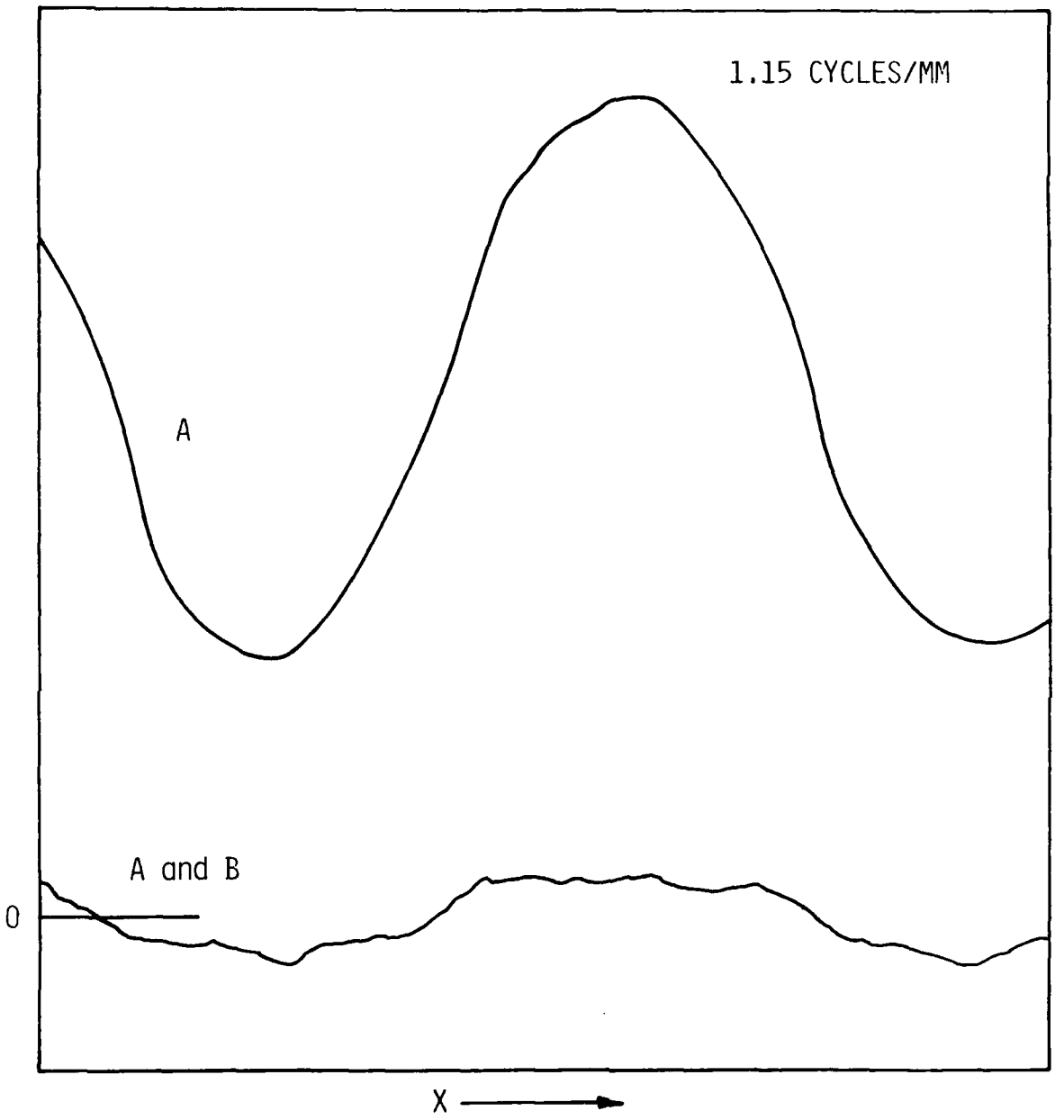

Figure 7. Sptaial scan at $\omega = 0.118\ \omega_c$.

Figure 8 shows spatial scans of a 5.75 cycle/mm ruling, which corresponds to 0.59 ω_c. The lower scan, made with the circular pupil alone, shows no significant modulation. This is to be expected, since the MTF for this pupil drops to zero well below this frequency. The levels of modulation in the upper two scans, with the annulus alone open and with both pupils open, are about equal, as would be expected.

Of the present shortcomings of the apparatus which limit the suppression ratio seen in Figure 7, one of the most important is probably nonuniform illumination of the entrance pupils by the test source. Among the possible causes of non-uniform illumination are mis-alignment of the condenser system in the source and non-uniformities from point to point in the relectance of the collimating mirror and two folding mirrors. The effect of such non-uniformities is to distort shapes of the MTF's from the nominal shapes which are shown in Figure 3. Then, in their distorted forms, they can still be forced to match at ω=0, but will in general be mismatched at all higher spatial frequencies. Various techniques are available to correct this situation. Diffusers could be added to the source, and various states of adjustment of the condenser optics could be tested to find the one which is most uniform. The mirrors involved could be re-coated. An incandescent lamp with a ribbon filament could be substituted for the present coil-type filament. Other possible problem areas are that the images through the two pupils may be spatially displaced due to wedging in the N-D filter or the half wave plate, or that the wavelength at which the half wave plate produces $\lambda/2$ retardation may not coincide adequately with the passband of the interference filter. These and other possible problem areas will be examined in the next phase of this program, and it is expected that substantially improved suppression ratios will be achieved in the future. The objective of the next phase will be to demonstrate suppression over the range of lower spatial frequencies by a factor of 100.

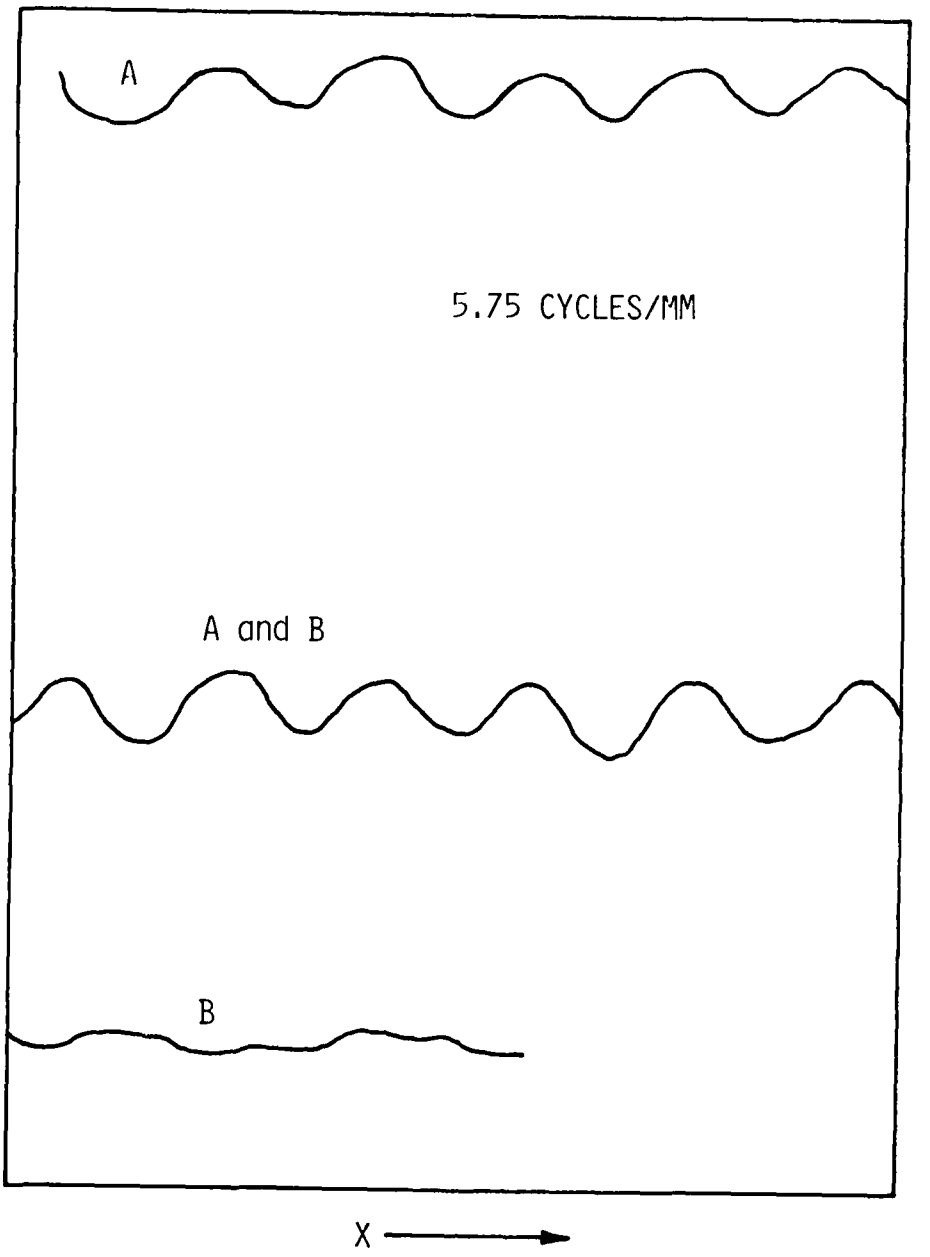

Figure 8. Spatial scan at $\omega = 0.59\ \omega_c$.

References

1. T. Zehnpfennig and G.A. Vanasse, SPIE Proceedings Vol. 156, 98 (1978).

2. T. Zehnpfennig, S. Rappaport, and G.A. Vanasse, SPIE Proceedings Vol. 191, 71 (1979).

3. O. Shepherd, W.P. Reidy, and G.A. Vanasse, SPIE Proceedings Vol. 191, 64 (1979).

4. T. Zehnpfennig, O. Shepherd, S. Rappaport, W.P. Reidy, and G.A. Vanasse, Appl. Opt. 18, 1996 (1979).

5. T. Zehnpfennig, S. Rappaport, and R. Wattson, SPIE Proceedings Vol. 253, 8 (1980).

6. T. Conley and O. Panfilov, SPIE Proceedings Vol. 268, (1981).

APPENDIX

Paper published in SPIE Proceedings Vol. 253

Reprinted from SPIE Vol. 253 - Modern Utilization of Infrared Technology VI
1980 by the Society of Photo-Optical Instrumentation Engineers, Box 10, Bellingham, WA 98225 USA

Background suppression with variable modulation transfer function (MTF) imaging systems

Theodore Zahnpfennig, Saul Rappaport, Richard Wattson
Visidyne, Incorporated, 5 Corporate Place, So. Bedford Street, Burlington, Massachusetts 01803

Abstract

A technique is described for suppressing the lower spatial frequencies in the object using an optical system with a time-varying MTF. The technique is applicable to imaging radiometers operating in the infrared region. The required variations in the MTF are produced by causing the image to move in a programmed sequence of small amplitude circular gyrations on the face of the detector. The gyrations are performed at a frequency high compared to the system frame rate. A series of calculations are described which indicate that, at low spatial frequencies, average suppression ratios of at least 500 to 1 can be achieved with this technique.

Introduction

This paper discusses a technique of background suppression on an optical level by means of suitably matched or tailored pairs of modulation transfer functions which, when subtracted from one another, suppress the lower spatial frequencies in the object scene. This, in turn, enhances the detectability of point sources or targets in the presence of structured backgrounds. The technique is intended to be applied to image-forming radiometers operating at or near the diffraction limit in the infrared region of the spectrum.

Figure 1 shows a somewhat idealized pair of modulation transfer functions of this type. The MTF labeled $T_A(\omega)$ initially drops steeply, then levels off, and finally falls to zero at the cutoff frequency, $\omega=1.0$. The MTF labeled $T_B(\omega)$ closely matches T_A out to $\omega\approx 0.3$. However, beyond this point, it continues to fall steeply, actually becoming negative (producing reverse contrast) over the range of higher spatial frequencies before returning to zero at $\omega=1.0$. When subtracted from one another, the resulting Net MTF (T_A minus T_B) results in effective suppression of the lower spatial frequencies, while the image contrast for those higher spatial frequencies which would characterize a point source is preserved or actually enchanced.

Previous work at Visidyne has concentrated on adapting this concept for use in background suppression imaging double-beam interferometers. (References 1, 2, 3, and 4). A double-beam interferometer is shown schematically in Figure 2. The device has two entrance apertures, at A_1 and A_2, and two outputs, at D_1 and D_2, where detector arrays can be placed. The two modulation transfer functions typically are defined by optical components or stops placed at these two entrance apertures. For each quarter-wave motion of the moving roof reflector M_1, the image formed on a given detector array is switched from radiation passing through one entrance aperture to that passing through the other entrance aperture. The two modulation transfer functions are, in effect, subtracted by detecting only the fluctuations in the image as the roof reflector is translated.

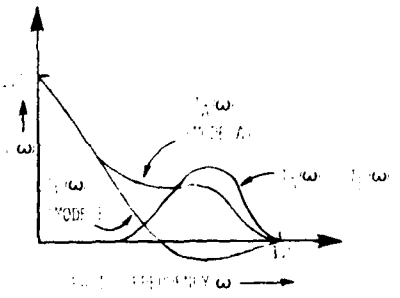

Figure 1. Idealized set of matched modulation transfer functions.

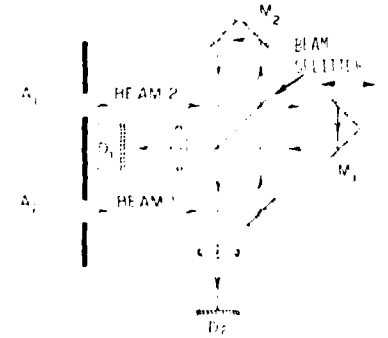

Figure 2. Schematic diagram of a double-beam interferometer.

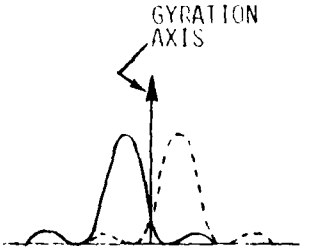

Figure 3. Instantaneous diffraction pattern gyrating about an axis approximately two-thirds of the way to the first dark ring.

BACKGROUND SUPPRESSION WITH VARIABLE MODULATION TRANSFER FUNCTION (MTF) IMAGING SYSTEMS

A number of techniques for tailoring the MTF of a given optical system to the desired form have been investigated. These include introducing controlled amounts of various geometrical aberrations into the system, slightly defocusing the system, adding central obstructions of various diameters to the entrance pupil, introducing optical path length changes of $\lambda/2$ over various areas of the pupil, and causing the image to undergo small amplitude circular gyrations at high frequency on the detector face. These techniques are described in more detail in the references.

Variable MTF radiometer

In the present work, we wish to adapt the tailored modulation transfer function concept to imaging radiometers, for applications where the high spectral resolution of an interferometer is not required or where the bulk and complexity of an interferometer is not wanted. The main problem here is that, unlike a double-beam interferometer, an imaging radiometer normally has only one entrance pupil and, at any moment in time, only one MTF. The concept could, however, be adapted to a radiometer if the optical properties of this single entrance pupil could be varied with time in order to switch from one MTF to the other. Thus, on alternate frames, the MTF of the radiometer would resemble that of I_A (Mode A) in Figure 1, and on the remaining frames it would resemble that of I_B (Mode B). By detecting only the image fluctuations, the net MTF would be the difference between the two instantaneous MTF's. To be practical, the changes in the MTF must be effected without major mechanical motions or major optical component changes. For these reasons, techniques involving various combinations of small amplitude gyrations of the image on the detector face appear to be most promising, and are examined in detail in this paper.

Figure 3 illustrates the type of gyrations which are of interest here. The solid curve represents the profile of the instantaneous diffraction pattern produced by the optical system. By translating and/or tilting one of the optical components in the system, this diffraction pattern is made to move in a circular motion about an axis which, in this case, is located part of the way out to the first dark ring. Thus, the dashed curve is the profile of the diffraction pattern one-half of a gyration cycle later. It will be shown that gyration radii no more than several times the radius of the first dark ring are sufficient to produce the required modifications in the MTF. Thus, the amplitude of the gyrations is very small, being on the arcsecond or sub-arcsecond level for any real set of optical system dimensions. The frequency of the gyrations must be high compared to the system frame rate, so that the observed MTF during any given frame will, in fact, be the time-averaged MTF. Typically, acoustical frequencies on the order of 10 kHz would be appropriate. The gyrations could be driven by existing types of actuators, such as a set of piezoelectric drivers. An advantage of the gyration technique for tailoring the modulation transfer functions is that, by controlling the actuators with a programmable function generator, the optical system characteristics can be adjusted on a software level. Thus, the radiometer can be considered to be an adjustable spatial filter whose filtering characteristics can be tuned at will. An additional advantage is that the effective collecting areas of the optical system in Modes A and B are automatically matched, since they time-share the same entrance pupil. Matched collecting areas are required for effective background suppression with this technique.

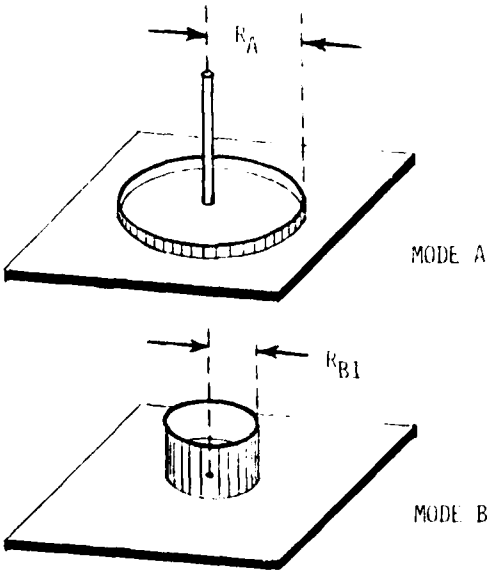

Figure 4. General pattern of gyrations giving modulation transfer functions similar to those of Figure 1.

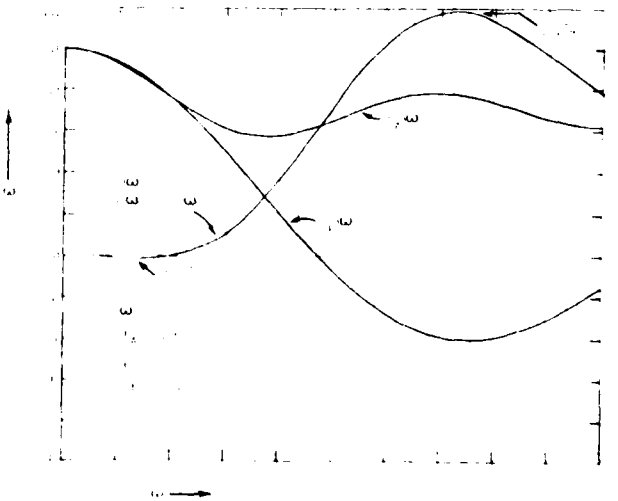

Figure 5. A set of MTF modifying functions for the gyration pattern shown in Figure 4.

Calculations of gyration radii and dwell times

In our initial calculations, we assumed that one MTF of the matched pair would be the MTF of a stationary or non-gyrated optical system, and that it would be similar in shape to $I_A(\cdot)$ in Figure 1. We then attempted to find a pattern of gyrations which would transform I_A into a time-averaged MTF similar to $I_U(\cdot)$. The result of this attempt was that some of the required gyrations would have to be performed for negative periods of time. We interpret this result to mean that I_A can not be the MTF of any stationary optical system, and that it also must be produced by applying a pattern of gyrations to some other stationary system with an MTF of $I_U(\omega)$.

A pattern of gyrations which was found to give pairs of modulation transfer functions of the desired form is shown in Figure 4. This figure illustrates the general form of the two distribution functions of the gyration radii. For those frame periods when the radiometer is to be in Mode A with an MTF of I_A, a fraction of the time is spent gyrating at a radius R_A, and the remainder of the time is spent dwelling at a gyration radius of zero, as shown. For the alternate periods when it is to be in Mode B with an MTF of I_B, the entire time is spent gyrating at some other radius R_{B1}. Thus, the distribution functions $b_A(r)$ and $b_B(r)$ for the gyration radii can be written as follows:

$$b_A(r) = f\cdot(r-0) + (1-f)\cdot(r-R_A) \tag{1}$$

$$b_B(r) = \cdot(r-R_{B1}) \tag{2}$$

where $(r-R)$ is the delta function in cylindrical coordinates, and f is the fraction of the time that the system spends dwelling at a gyration radius of zero when it is in Mode A. As it is used here, the delta function in cylindrical coordinates is defined to have the following property:

$$\int \cdot(r-R)dr = 1/2\pi R. \tag{3}$$

In the calculations described here, the transition times in switching from one gyration radius to another have been assumed to be negligible, and their effects on the MTF have been neglected.

The time-averaged point spread function of the gyrated optical system is the stationary point spread function convolved with the distribution function b(r) of gyration radii. Thus, the gyrated MTF, $I(\cdot)$, is the product of the stationary MTF, $I_U(\cdot)$, and the Fourier Transform $B(\cdot)$ of $b(r)$:

$$I(\cdot) = I_U(\cdot)\, b(\cdot). \tag{4}$$

Then, the modulation transfer functions of for Modes A and B are given by:

$$\begin{aligned} I_A(\cdot) &= I_U(\cdot)\, b_A(\cdot) \\ &= I_U(\cdot)\, 2\pi \int b_A(r)\, J_0(2\pi r\omega)rdr \\ &= fI_U(\cdot) + (1-f)\, I_U(\cdot)\, J_0(2\pi R_A\cdot) \end{aligned} \tag{5}$$

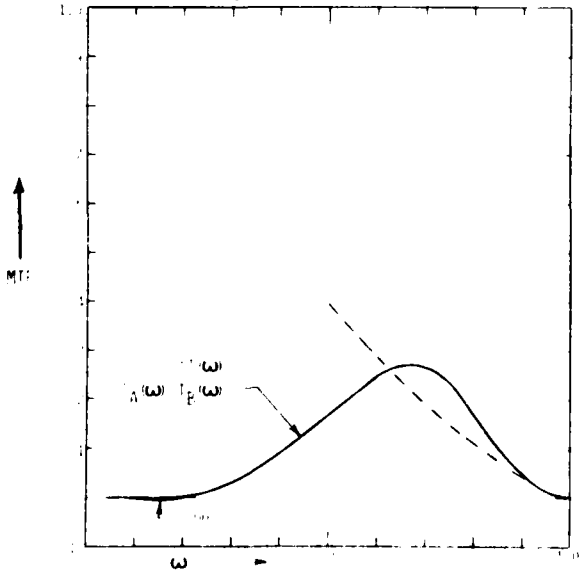

Figure 6. The net MTF, $I(\cdot)$, found by multiplying the MTF of a diffraction limited annulus by $I(\cdot)$ from Figure 5.

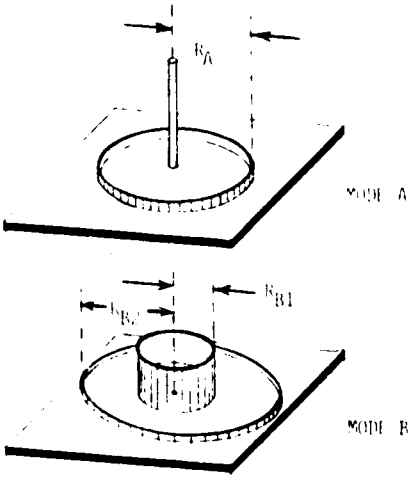

Figure 7. Gyration patterns with an additional gyration radius R_{B2} added to Mode B.

$$I_B(\omega) = I_0(\omega)\, F_B(\omega) = I_0(\omega)\, J_0(2\pi R_{B1}\omega) \tag{6}$$

Here, J_0 is the zero order bessel function. If we require that I_A and I_B match at some spatial frequency ω_0 (as well as at $\omega=0$), the condition for matching can be found by combining equations 5 and 6:

$$J_0(2\pi R_{B1}\omega_0) = f + (1-f)\, J_0(2\pi R_{A1}\omega_0). \tag{7}$$

Note that equation 7 does not depend on the stationary MTF, I_0. Thus, when this equation is satisfied, I_A and I_B will match at $\omega=0$ and $\omega=\omega_0$ regardless of the stationary MTF which was chosen. For this reason, it was considered to be more significant to calculate, initially, a pair of MTF modifying functions $F_A(\omega)$ and $F_B(\omega)$ rather than I_A and I_B. Here:

$$I_A(\omega) = F_A(\omega)\, I_0(\omega) \tag{8}$$

$$I_B(\omega) = F_B(\omega)\, I_0(\omega). \tag{9}$$

Once F_A and F_B are known, then any desired I_0 can be selected, and the pair of gyrated modulation transfer functions can be calculated.

Holding ω_0 fixed at 0.20, a series of calculations of I_A and I_B were made by varying the gyration radii R_A and R_B over a grid-like search pattern. Regions of the grid pattern yielding the best forms for F_A, F_B, and the difference $\Delta I = I_A - I_B$ were explored in detail. The criterion for selecting the best forms was that ΔI remain as close to zero as possible from $\omega=0$ to $\omega=0.20$, and then that it climb to as large a value as possible between $\omega=0.50$ and $\omega=0.80$. The results of one of the calculations in this series are shown in Figure 5. Here, the gyration radii R_A and R_B were 1.615 and 0.808, respectively. (Here, the units of the gyration radii are λ/b radians. Thus, a value for R_B of 0.808 corresponds to gyration about an axis which is $0.808/1.22 = 66\%$ of the way to the first dark ring in the diffraction pattern for a circular aperture of diameter b.) A dependent variable in the calculation was f, the fraction of the time spent in dwelling at a radius of zero when the system is in Mode A. Here, f was 0.655. I_A and I_B are seen to match quite well from $\omega=0$ to $\omega=0.20$, with a maximum mismatch of -.0127 at $\omega=0.15$. Beyond this point they diverge, reaching a maximum difference ΔI of 1.174 at $\omega\approx0.75$. Thus, at this spatial frequency, the net MTF would actually be enhanced over the stationary MTF by about 17%.

In Figure 6, the function ΔI from Figure 5 has been multiplied by the MTF of a stationary, diffraction limited annular aperture having a central obstruction equal to 50% of its diameter. (An annular aperture was chosen here because any actual optical system of this type would probably have a secondary mirror, and also because the steeply falling MTF of an annulus helps to reduce the deviation of the net MTF from zero between 0.6 and 0.8.) The resulting net MTF, ΔI, shows effective background suppression out to $\omega=0.20$, with a maximum deviation from zero of -.008 at $\omega=0.15$. At spatial frequencies beyond 0.6, the net MTF shows considerable enhancement over that of a diffraction limited circular aperture, which is indicated by the dashed line in this figure.

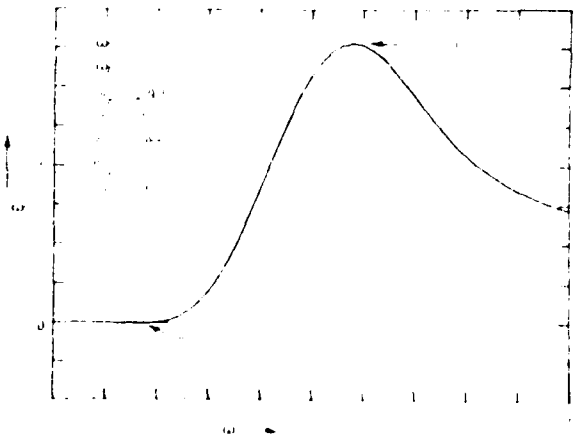

Figure 7. An MTF modifying function for the gyration pattern shown in Figure 7.

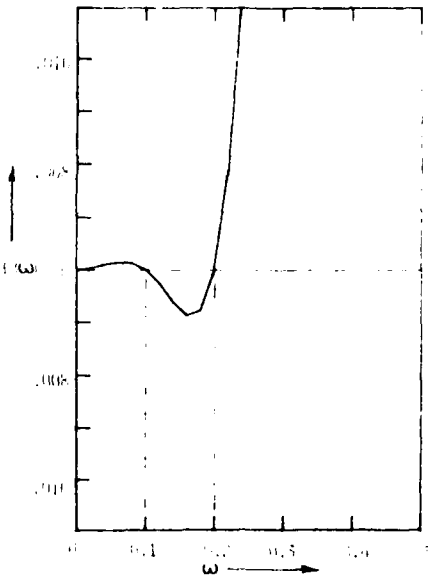

Figure 8. $\Delta I(\omega)$ from Figure 8, with the ordinate scale expanded to show the behavior of the function at low spatial frequencies.

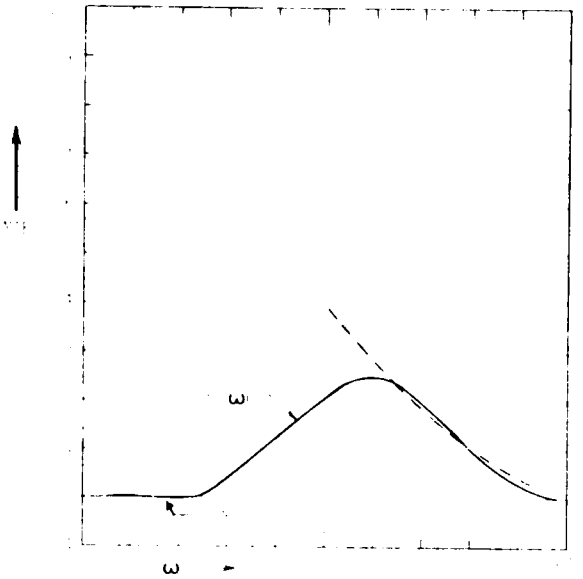

Figure 10. The net MTF found by multiplying the MTF of a diffraction limited annulus by MF( ) from Figure 8.

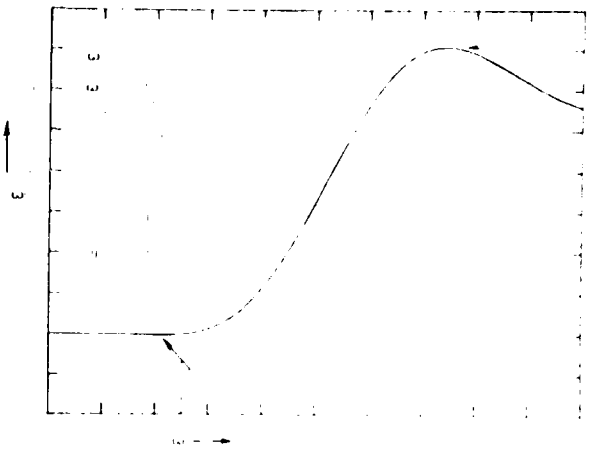

Figure 11. An MTF modifying function with the region of effective background suppression extended to higher spatial frequencies.

If the general pattern of gyrations is restricted to the form shown in Figure 4, then the MTF modifying functions in Figure 5 are probably the optimum or near-optimum set which can be found. In order to obtain further improvements in background suppression at lower spatial frequencies while retaining good response at the higher frequencies, an additional degree of freedom is needed in the gyration pattern. We have required that the optical system in Mode A alternate between two gyration radii: zero and K_A. Therefore, requiring the system in Mode B to alternate between two gyration radii as well is probably not a serious additional complication. Figure 7 shows the general pattern of gyration radii with this additional gyration radius K_{b_2} added to Mode B. The gyration distribution function for Mode B then becomes:

$$h_B(r) = g\,\delta(r-K_{b_1}) + (1-g)\,\delta(r-K_{b_2}) \qquad (1)$$

where g is the fraction of the time the system spends gyrating at K_{b_1} when it is in Mode B. With the additional degree of freedom provided here, it is possible to match f_A and f_B at some other spatial frequency ν_b in addition to the previous ν_b. Then, the condition for matching previously given in Equation will be replaced by the following two expressions:

$$g\,\omega_0(2\pi K_{b_1}\nu_b) + (1-g)\,\omega_0(2\pi K_{b_2}\nu_b) = f + (1-f)\,\omega_0(2\pi K_A\nu_b) \qquad (2)$$

$$g\,\omega_0(2\pi K_{b_1}\nu_L) + (1-g)\,\omega_0(2\pi K_{b_2}\nu_L) = f + (1-f)\,\omega_0(2\pi K_A\nu_L) \qquad (3)$$

For convience in our further calculations, we set ν_L equal to $\nu_b/2$.

Sets of MTF modifying functions were calculated for various combinations of K_{b_1}, K_{b_2}, and K_A. The results for one of these combinations are shown in Figure 8. Here ν_b was set equal to 0.20, and thus ν_L = 0.10. Note that, with the added degree of freedom, the low spatial frequency characteristics of ZF are substantially improved over Figure 5, with the maximum deviation from zero below ν_b being reduced from -0.127 to -0.035. In Figure 9, the ordinate scale of Figure 8 has been expanded to show details of the behavior of ZF at low spatial frequencies. In Figure 10, the MTF of the previously described annulus has been folded in, showing the net MTF of the optical system. Again the dashed line shows, for comparison, the MTF of a diffraction limited circular aperture. The maximum deviation from zero below ν_b of -0.02 indicates that, in theory, average suppression ratios of 500 to 1 or greater are possible over the low spatial frequency range with this technique. Attempting to improve the theoretical suppression ratio beyond this point was not considered to be worthwhile, since actual suppression ratios will probably be limited to values of this order by such things as optical component tolerances, alignment tolerances, and the effects of the finite transition time needed to switch from one gyration radius to another.

If desired, the region of effective background suppression can be extended to higher spatial frequencies. In Figure 11, ν_b has been raised to 0.25. The resulting MTF modifying function indicates that spatial frequencies out to ν=0.50 or 0.35 would be effectively suppressed.

Implementation of the technique

Two ways in which this background suppression technique could be implemented are shown schematically in Figure 12. A Cassegrain optical configuration is indicated here, although in fact it might be a Schmidt system or some other catadioptric configuration. In any case, the system would probably include a secondary mirror. In Figure 12a, the secondary mirror is mounted on a set of piezoelectric actuators which produce the required gyrations of the image on the face of the detector array by wobbling the secondary so that its optical axis traces out a circular cone with time. This motion of the secondary will also tilt the image plane with respect to the detector face. However, since the gyrations are to be on the arcsecond or sub-arcsecond level, the resulting defocusing of regions of the image will be negligible. In Figure 12b, the secondary mirror is fixed, and the actuators are used to drive a planar mirror located just in front of the detector array. The driven mirror in this configuration would probably be smaller and less massive than the driven mirror in Figure 12a, although the amplitude of the motions would have to be greater because of the shorter optical path to the detector. As indicated, the actuators would be driven by a programmable function generator. The function generator would produce waveforms of the type $+A \sin \omega t$ and $\pm A \cos \omega t$, where the amplitude A would correspond to the particular gyration radius required at any given moment.

Conclusions

The calculations described here indicate that very effective suppression of the lower spatial frequencies in an object scene can be obtained on an optical level in single-pupil systems with a technique which requires only microscopic motions of one of the optical components. The actual suppression ratios which can be achieved will probably be limited by component and alignment tolerances, and by the finite time required to switch from one gyration radius to another. However, we expect that the effects of some of these practical limitations can be diminished by fine tuning the system by means of minor adjustments in the gyration radii and the dwell times. A laboratory measurements program to evaluate this technique is presently being conducted.

This work was supported in part by the Air Force Space Division and the Air Force Geophysics Laboratory under Contract F19628-79-C-0005.

References

1. J. Zehnpfennig and G. Vanasse, SPIE Proceedings Vol. 156, 98 (1978).
2. J. Zehnpfennig, S. Rappaport, and G. Vanasse, SPIE Proceeding Vol. 191, 71 (1979).
3. G. Shepherd, W.P. Reidy, and G. Vanasse, SPIE Proceedings Vol. 191, 64 (1979).
4. J. Zehnpfennig, G. Shepherd, S. Rappaport, W. Reidy, and G. Vanasse, Appl. Opt. 18, 1996 (1979).

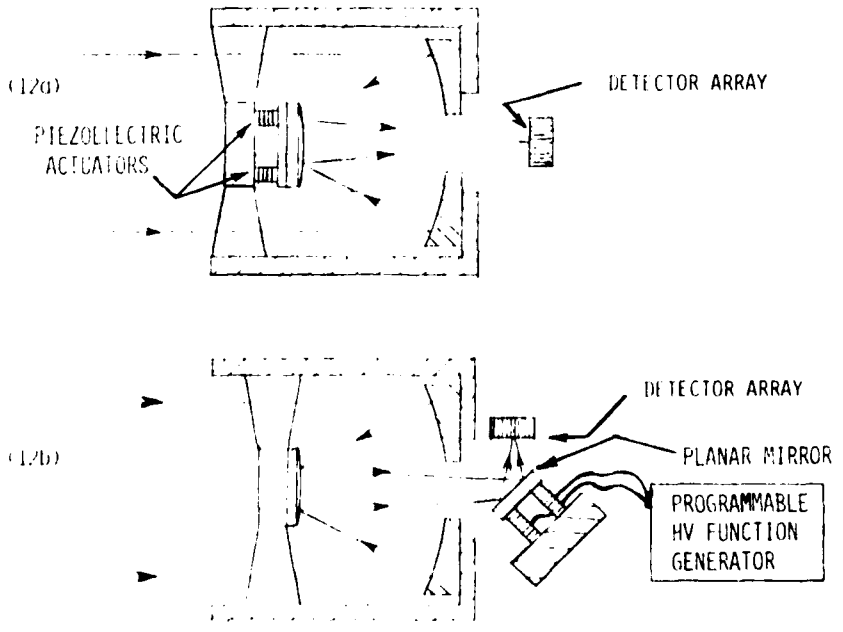

Figure 12. Implementation of the variable MTF technique.

Question

If the spatial filtering technique described were to be applied to detecting moving targets, would you propose following it with the usual temporal filtering techniques suggested, such as frame to frame subtraction?

T. Janssens
Aerospace Corporation

Answer

Generally, one would want to take advantage of all the relevant techniques which would improve the detection process. The variable MTF technique used in conjunction with frame to frame subtraction may make the latter easier to implement, since most of the background is eliminated prior to using frame to frame subtraction. That is, it may decrease the precision with which frame to frame subtraction must be performed in order to reach a given overall level of background suppression.

Question

Does this system cope only with circularly symmetric types of backgrounds, or does it cope equally well with an edge or other non-symmetric features?

Answer

It is not limited to circularly symmetric features. The background suppression characteristics are isotropic, and do not depend on the orientation of the spatial frequencies which make up a given feature in the object. This is one advantage of this type of spatial filter over types using grilles or reticles, which generally have a preferiental direction.

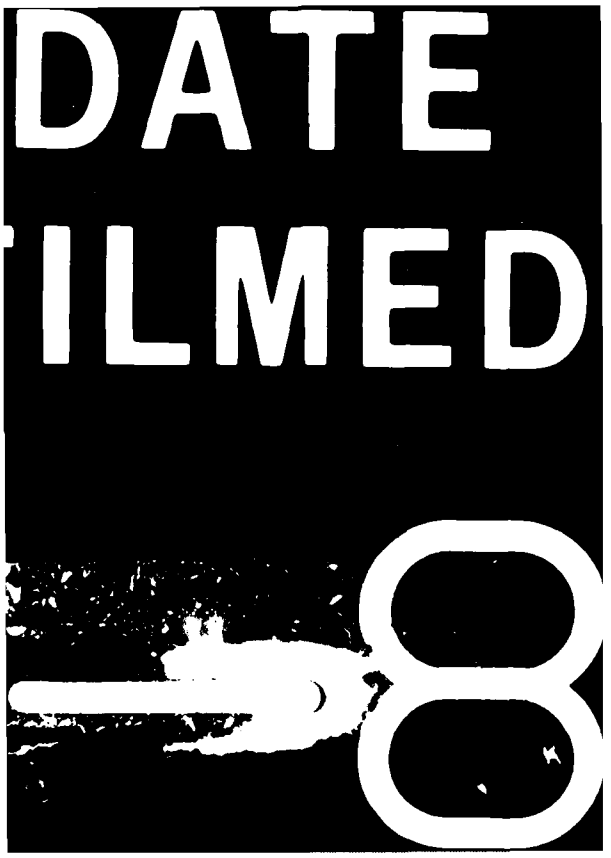
DATE
ILMED
8